Received: 24 September 2019 | Revised: 27 December 2019 | Accepted: 31 December 2019
DOI: 10.1002/jbma.a.36875

ORIGINAL ARTICLE

Self-assembled biomimetic Nano-Matrix for stem cell anchorage

Libo Zhou[1] | Anne Yau[1,2] | Hongchuan Yu[2] | Liisa Kuhn[1,3] | Wei Guo[4] | Yupeng Chen[1,2]

[1]Department of Biomedical Engineering, University of Connecticut, Storrs, Connecticut
[2]Brown University Medical School, Providence, Rhode Island
[3]Department of Biomedical Engineering, University of Connecticut, Farmington, Connecticut
[4]Beijing Friendship Hospital, Capital Medical University, Beijing, China

Correspondence
Yupeng Chen, Department of Biomedical Engineering, University of Connecticut, 260 Glenbrook Road, Unit 3247, Storrs, CT 06269-3247
Email: yupeng.chen@uconn.edu

Funding information
NCF Career Award, Grant/Award Number: 1653702; University of Connecticut; National Institutes of Health (NIH), Grant/Award Numbers: 1R03AR069383-01, 1R01AR072027-01

Abstract
Mesenchymal stem cells (MSCs) have been widely applied in biomedicine due to their ability to differentiate into many different cell types and their ability to synthesize a broad spectrum of growth factors and cytokines that directly and indirectly influence other cells in their vicinity. To guide MSC infiltration to a bone fracture site, we developed a novel self-assembled Nano-Matrix which can be used as an injectable scaffold to repair bone fractures. The Nano-Matrix is formed by Janus base nanotubes (JBNTs) and fibronectin (FN). JBNTs are nucleobase-derived nanotubes mimicking collagen fibers, and FN is one of the cell adhesive glycoproteins which is responsible for cell–extracellular matrix interactions and guides stem cell migration and differentiation to desired cells types. Here, we demonstrated the successful fabrication and characterization of the JBNT/FN Nano-Matrix as well as its excellent bioactivity that encouraged human MSC migration and adhesion. This work lays a solid foundation for using the Nano-Matrix as an injectable approach to improve MSC retention and function during bone fracture healing.

KEYWORDS
anchorage, fibronectin, Janus-based nanotubes, mesenchymal stem cells, Nano-Matrix

1 | INTRODUCTION

Osteoporosis is a common and frequently occurring disease, and the fractures that occur in patients with osteoporosis not only cause great pain and are slow to recover from, but also bring a heavy economic burden to the patients. Approximately 54 million people in North America are diagnosed with low bone density and are at risk of fracture. Even worse, about 8.9 million suffer from fractures worldwide (Johnell & Kanis, 2006). Bone fracture healing is difficult especially for older, as well as osteoporotic, patients because of age-related reductions in bone formation and age-related increases in bone resorption (Gibon, Lu, & Goodman, 2016). The older the patient, the lower activity of the osteoblast. The decreased activity of osteoblasts is one of many reasons for delayed healing of bone fractures in older patients (Manolagas & Parfitt, 2010). Activation and migration of mesenchymal stem cells (MSCs) have been shown to play an important role in fracture healing (Yao et al., 2016) and are also decreased with age (Sui, Hu, Zheng, & Jin, 2016).

MSCs have been proven to have strong immunosuppressive properties with the ability for self-renewal and self-differentiation (Yao et al., 2016). The presence of MSCs has been shown to promote angiogenesis, increase tissue repair and reduce inflammation, which is important in wound healing (Hadjiargyrou & O'Keefe, 2014). Under the correct conditions, MSCs differentiate and participate in endochondral ossification to form bone in the gaps of the fractured bones (Karp & Leng Teo, 2009). While they have the potential to differentiate into a tissue-specific cell type, they could differentiate to an undesired cell type, such as a fibroblast, which promotes scarring instead of regeneration of the damaged tissue (van den Bogaerdt et al., 2009). It has been a challenge to promote and guide endogenous MSCs to

Libo Zhou and Anne Yau contributed equally to this study.

the fracture site and to promote adhesion and function at the target location.

As attracting MSCs to migrate into and adhere within the fracture site is the first step in bone regeneration, a successful tissue engineering scaffold should be able to enhance stem cell anchorage which includes supporting migration and adhesion. This is the prerequisite for cell differentiation and function. Without a biomaterial or biochemical cues to guide them, only a small portion of injected MSCs reaches the target tissue and remains at the desired location, especially in the case of systemic administration (De Becker & Riet, 2016). Although variously engineered scaffolds have been used to facilitate MSCs migration and adhesion, some fracture locations (such as a growth plate fracture in the middle of a long bone) are not easy to access and do not readily accommodate conventional grafting materials or scaffolds which are prefabricated. Moreover, prefabricated scaffolds may not fit perfectly into an irregularly shaped fracture. Therefore, we have developed a nanomaterial that is not only biomimetic but can self-assemble in situ and thereby be injectable directly into the target area.

In the present study, we fabricated a novel Nano-Matrix composited of Janus base nanotubes (JBNTs) and fibronectin (FN) that will ideally guide the migration of host endogenous progenitor cells into the fracture. JBNTs are derived from DNA base pairs (Chen, Song, Yan, Fenniri, & Webster, 2011; Fenniri et al., 2001; Song, Chen, Yan, Fenniri, & Webster, 2011), specifically adenine and thymine in our case. As seen in Figure 1, six derived DNA base pairs molecules can bond to form a plane by self-assembly via hydrogen bonding. These planes are then stacked on each other via a strong pi-stacking interaction to fabricate a nanotube which can be up to 200–300 μm in length. The inner hydrophobic hollow channels of the nanotube are approximately 3.5 nm in diameter and can be used for drug encapsulation (Danial, Tran, Young, Perrier, & Jolliffe, 2013).

FN is a ubiquitous adhesive glycoprotein, which is found in the extracellular matrix (ECM) alongside with collagen and other glycoproteins such as laminin (van den Bogaerdt et al., 2009). These glycoproteins are multidomain proteins with different binding sites for integrins, collagens, and other ECM proteins (Veevers-Lowe, Ball, Shuttleworth, & Kielty, 2011). The JBNTs are designed to morphologically mimic collagen fibers so that FN can react with them via noncovalent bonding. This Nano-Matrix can self-assemble in water in a few seconds without using any chemical initiators, heat source, or ultraviolet (UV) light, enabling it to be injected into a bone fracture site that is not accessible by conventional grafting materials or prefabricated scaffolds. Our studies demonstrate that the self-assembled biomimetic Nano-Matrix creates a microenvironment which has positive effects on MSC cell differentiation and cell adhesion.

2 | METHODS

2.1 | Materials

JBNTs were synthesized by an effective approach published previously (Chen, Yu, & Chen, 2017). Human MSCs (hMSCs) (containing ≥750,000 cells/vial), Stem Cell Growth Medium BulletKit, and Tritc-phalloidin were purchased from Lonza. Trypsin–EDTA solution (Gibco, 0.25%), phosphate buffered saline (PBS, Gibco), GlutaMAX media (Gibco), fetal bovine Solution (FBS, Gibco), Penicillin–Streptomycin (Gibco, 10,000 U/ml), and Triton X-100 (Invitrogen, 1.0%) were purchased from Thermo Fisher. Formalin and Ethanol (70% solution) were obtained from Fisher Scientific. Then, 12-well, 24-well, and 96-well clear round-bottom microplates were obtained from Corning. The catalog numbers of these plates are 353043, 353047, and 353,072, respectively. The 8-μm cell insert also was obtained from corning, the catalog number is 353182. The 8-well cell culture slides were purchased from Thermo Fisher, and the catalog number is 155409. FN (1.0 mg/ml) came from Gibco, and its catalog number is PHE0023.

2.2 | Fabrication of Nano-Matrix

For material development and characterization, the FN, JBNTs, and Nano-Matrix were coated on the bottoms of wells of a 96 wells plate, and then we carried out the experiments as follows. Three solutions were prepared: FN, JBNT, and FN + JBNT. FN (30 μl of 100 μg/ml water solution) were diluted in 150 μl Milli-Q water to make a 20 μg/ml solution of FN. JBNTs (15 μl of 1 mg/ml JBNT water solution) were added into 150 μl Milli-Q water to make a 100 μg/ml of JBNTs. FN (30 μl of 100 μg/ml) and JBNTs (15 μl of 1 mg/ml) were mixed together in 150 μl water to form the solution denoted Nano-Matrix. Each of three wells of a 96-well plate received 50 μl of one type of solution (e.g., FN, JBNTs, and Nano-Matrix). The plate was

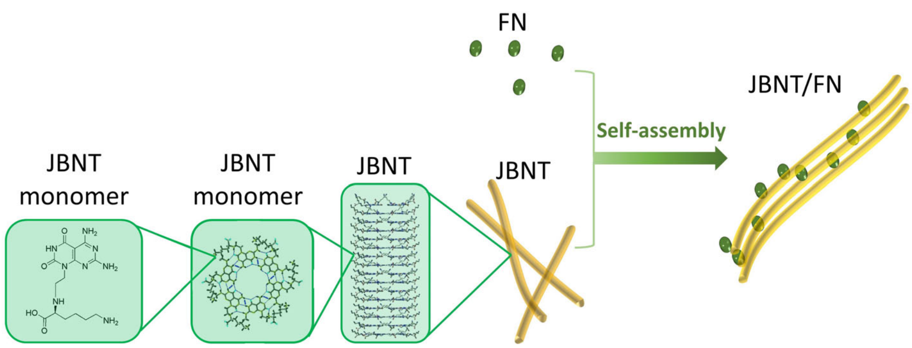

FIGURE 1 Schematic illustration of the hierarchical self-assembly of Janus base nanotubes (JBNTs) with a lysine side chain

frozen at −80°C and lyophilized overnight. The FN, JBNTs, and resulting self-assembled Nano-Matrix were characterized by light microscopy.

In other experiments, JBNTs in an aqueous solution (80 μl of 1 mg/ml) was added into the FN aqueous solution (40 μl of 1 mg/ml) and pipetted for several times. A white solid suspension was produced immediately after the addition of the JBNTs into the solution of FN. A video recording was made to capture the process of self-assembly.

2.3 | Characterization of the Nano-Matrix

2.3.1 | Absorption spectra measurement

For this measurement, FN (30 μl of 100 μg/ml) was mixed with MilliQ water (15 μl) and JBNTs (5 μl of 1 mg/ml) to form a Nano-Matrix solution. The final concentrations of FN and JBNTs in the Nano-Matrix solution were 60 and 100 μg/ml, respectively. Control solutions of FN and JBNT at these concentrations were also prepared. The UV–visible (Vis) absorption spectra were recorded for each solution with a NanoDrop (ThermoFisher).

2.3.2 | Transmission electron microscope

Plasma Cleaner Harrick Plasma PDC-32G was used to clean the grids before negative staining. Two negative staining processes were carried out for the specimens:

1. JBNTs aqueous solution (3 μl of 1 mg/ml) and JBNT/FN Nano-Matrix solution (3 μl) were each dropped on separate grids and left for 2 min before rinsing with 100 μl uranyl acetate (UA) solution (0.5%) by pipetting on the solution. The excess solution was removed from the grids with filter paper and then dried in air.
2. JBNT/FN Nano-Matrix aqueous solution (9 μl) was mixed with UA aqueous solution (3 μl, 2.0%) and pipetted for several times. The mixed solution was dropped on the grids and left for 2 min without further rinsing steps. The excess solution was removed from the grids with filter paper and then dried in air. Specimen characterization was carried out with the Lab6 20–120 kV transmission electron microscope (TEM).

2.4 | In vitro analysis methods

2.4.1 | Cell adhesion

Negative controls (NCs, no additives), JBNTs, FN and the JBNT/FN Nano-Matrix solutions were added into 24-well cell culture plates (1 ml for each well), respectively, and air-dried to be prepared as cell adhesion medium. Then, 10,000 cells/wells hMSCs were added into cell culture plates and incubated at 37°C, 5% CO_2 in DMEM media with 10% FBS. After culturing 24 hr, the medium in the wells were drained and the cell culture plates were rinsed with PBS solution. Then, cells were fixed with formalin and cell adhesion density was calculated by averaging the cell counts of five to nine random areas in each cell culture wells.

2.4.2 | Cell migration

A transwell method was used to determine cell migration on the Nano-Matrix. Briefly, an 8-μm cell insert was placed in a well of a 12-well plate. A total volume of 65 μl JBNT/FN Nano-Matrix assembled as described, was then added onto the transwell insert and coated in a 37°C incubator for 2 hr. Then, 0.5 million cells were added on top of the filter membrane in a transwell insert and incubated for 10 min at 37°C and 5% CO_2 in DMEM media with 10% FBS to allow the cells to settle. Then, 600 μl cell culture medium was gently added into the bottom well of the cell culture plate. After culturing 24 hr, the medium in the wells was removed and the cell culture plates were rinsed with PBS solution. Then, cells were fixed with formalin and the cell adhesion density was calculated by averaging the cell counts of five to nine random areas in the cell culture wells.

2.4.3 | Cell imaging and morphology analysis

Using the same method mentioned above, cells were culture on JBNTs, FN or JBNT/FN in 8-well cell culture slides at 37°C, 5% CO_2 in DMEM media with 10% FBS (0.5 ml per well). After 24 hr, the media in the wells were drained and the cell culture slides were rinsed with PBS solution three times. Cells were fixed with formalin, treated with Triton-X, and stained with Rhodamine. Cell images were captured with a fluorescence microscopy. Then, the images were analyzed using ImageJ image analysis software. Cell roundness and circularity were measured to observe the morphological changes of the stem cells. The software was calibrated to the image to convert pixels to μm or cm^2.

2.4.4 | Statistics

Data were expressed as the mean ± *SD*. Statistics were performed using a student one-tailed *t* test, followed by analysis of variance with $p < .05$ considered statistically significant.

3 | RESULTS

Our results showed that the assembly of Nano-Matrix from JBNTs and FN is very fast (in ~10 s). As shown in Figure 2, white scaffolds were obtained when the transparent JBNTs solution were mixed with the transparent FN solution by simply pipetting a few times. Interestingly, the formation of Nano-Matrix did not require any chemical initiator, UV light or organic solvents. Different from other emerging biomaterials where fabrications are based on external stimuli (such as UV light for crosslinking) (Jones & Leroux, 1999), Nano-Matrix is self-assembled in water without additives. The formed Nano-Matrix is flexible and injectable as shown in our Supplement Video S1. It can easily pass through a 200 μl pipette tip.

Bright-field images of FN, JBNTs, and the Nano-Matrix were captured and analyzed (Figure 3). The short clusters shown in Figure 3a consisted of FN only, indicating that the presence of FN alone cannot form a scaffold with long fibers and dense matrix. The short white spots observed in the FN group were the protein agglomerations. The thinner strands observed in Figure 3b indicated the presence of JBNTs. As shown in Figure 3c, the Nano-Matrix presented macrosized fibers which are visible by camera photos, while it also consisted of nanofeatured fibers shown in Figure 5. Compared to JBNTs, the Nano-Matrix had wider and longer fibers indicating that it is formed by crosslinking of JBNTs and FN. The macrosized Nano-Matrix fibers can grow up to several centimeters in length (Figure 3c).

UV–Vis spectra further indicated and characterized the assembly between JBNTs and FN. JBNTs has two absorption peaks at 220 and 280 nm, which are considered to be from the side chain and the aromatic rings of Janus, respectively. When assembled into Nano-Matrix, the value of the two peaks went down significantly due to the noncovalent binding of JBNTs and FN (Figure 4).

To characterize the morphological and structural difference of the JBNTs and Nano-Matrix, TEM analysis was completed. The JBNTs are slender tubes with uniform diameters (Figure 5a). Under neutral conditions, JBNTs and FN are positively and negatively charged, respectively, driving their complexation via charge interactions. As shown in Figure 5b, JBNTs bonded with FN tightly and formed long fibroid Nano-Matrix. When Nano-Matrix was preserved in a solution with low pH (4.0), it started to disassemble to release incorporated FN (Figure 5c). This is mainly because when pH dropped below the isoelectric point of the FN (pI = 5.5–6.0), FN became neutral or positively charged, leading to the Nano-Matrix bundles disassembly. As shown in Figure 5c, there were a lot of FN alongside the nanotube when the Nano-Matrix disassembled, which is also an evidence that the Nano-Matrix was composed by FN and JBNTs (Erickson, Carrell, & McDonagh, 1981).

Cell adhesion density is one of the in vitro parameters used for analysis of the experiment. It is shown that the stem cell adhesion of the Nano-Matrix group increased significantly (p-value <.05) compared to the negative control (Figure 6). This is mainly because the JBNT/FN Nano-Matrix are morphologically mimicking ECM, which

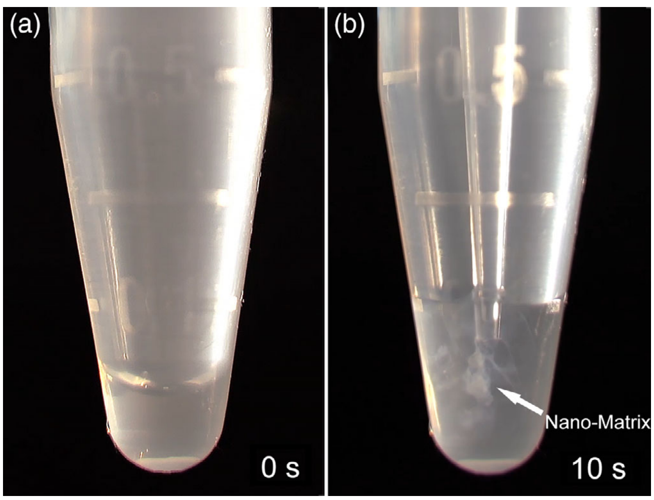

FIGURE 2 Demonstration for the self-assembled process of the Nano-matrix. (a) Fibronectin (FN) solution. (b) Janus base nanotubes (JBNTs) mixed with FN

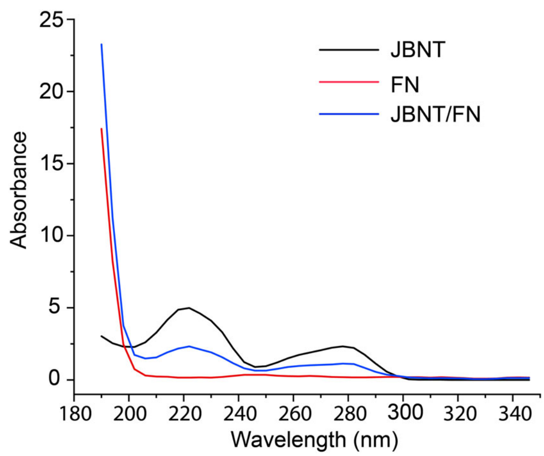

FIGURE 4 Absorption spectra of fibronectin (FN), Janus base nanotubes (JBNTs), and JBNT/FN Nano-Matrix

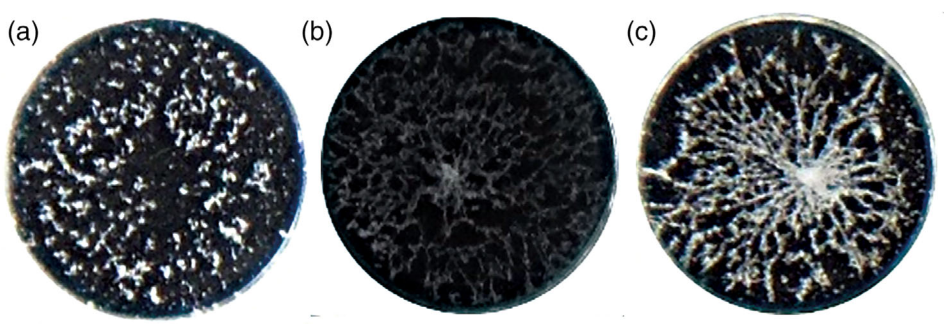

FIGURE 3 Bright-field photographs of (a) fibronectin (FN), (b) Janus base nanotubes (JBNTs) and (c) Nano-Matrix formed by JBNTs and FN. Each area has a diameter of 2 cm

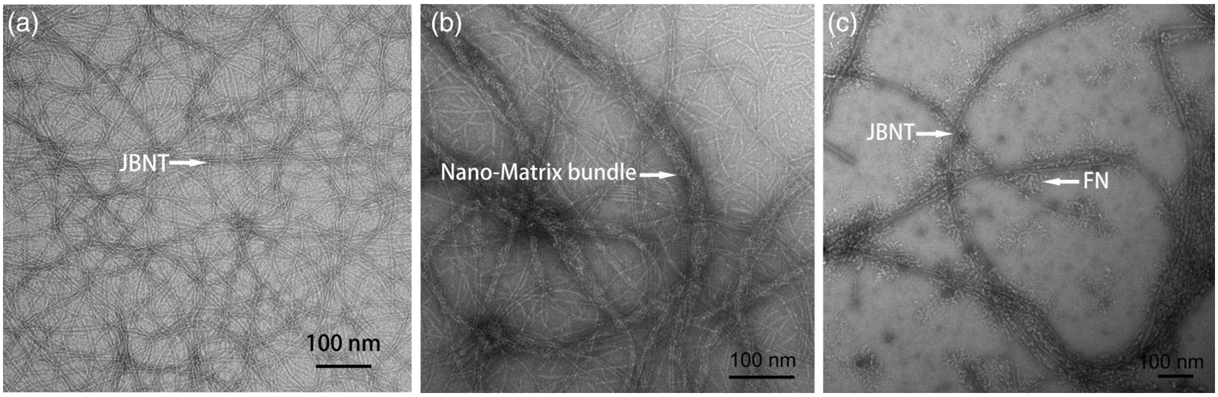

FIGURE 5 TEM images of (a) Janus base nanotubes (JBNTs), (b) JBNT/fibronectin (FN) Nano-Matrix, and (c) released JBNT/FN Nano-Matrix

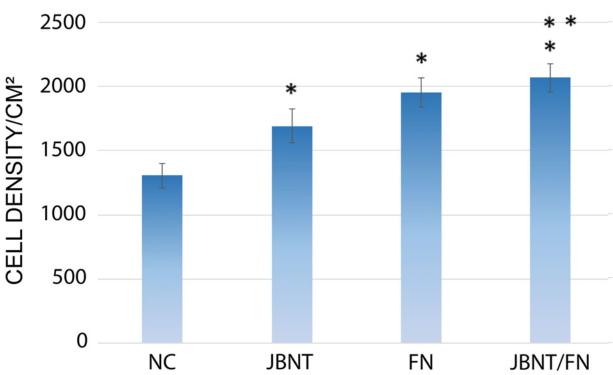

FIGURE 6 Statistical analysis of cellular adhesion. Cell adhesion density was recorded in this experiment. *$p < .01$ compared to negative controls. **$p < .05$ compared to Janus base nanotube (JBNT) alone. $N = 3$

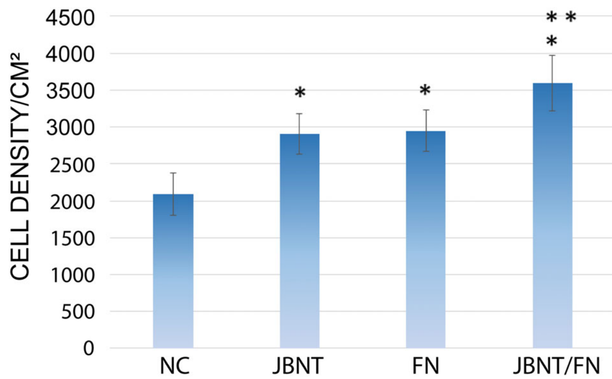

FIGURE 7 Statistical analysis of cell migration. *$p < .01$ compared to negative controls. **p < .05 compared to Janus base nanotube (JBNT) or fibronectin (FN) alone. $N = 3$

composed of collagens and cell adhesive glycoproteins such as FN (Martino et al., 2009). ECM determines tissue construction by providing a scaffold for cell adhesion (Singh & Schwarzbauer, 2012). Collagens have been shown to promote higher adhesion, survival and proliferation of MSCs (Somaiah et al., 2015). Additionally, FN, also has been shown to increase the cell adhesion of MSCs in the injured site (Martino et al., 2009). In adult stem cells, FN can promote differentiation along skeletal lineages while suppressing adipogenic differentiation, as well as enhancing MSCs migrations (Ogura et al., 2004).

In addition to cell adhesion, we also explored the effect of the Nano-Matrix on cell migration. As shown in Figure 7, JBNT/FN Nano-Matrix significantly enhanced hMSC migration. This may because that the JBNT/FN Nano-Matrix enhanced the focal adhesion between the substrate, cell membrane, and filopodia, which is critical for cell migration (de Barros et al., 2010). Fluorescence imaging of the hMSC also demonstrated that the Nano-Matrix significantly enhanced the cell adhesion better than negative control group (Figure 8 and Supplement Figure S1). Furthermore, the morphology of the hMSCs appears changed after incubated with the JBNT/FN Nano-Matrix. Cell morphology analyses were carried out to explore the effect of the Nano-Matrix.

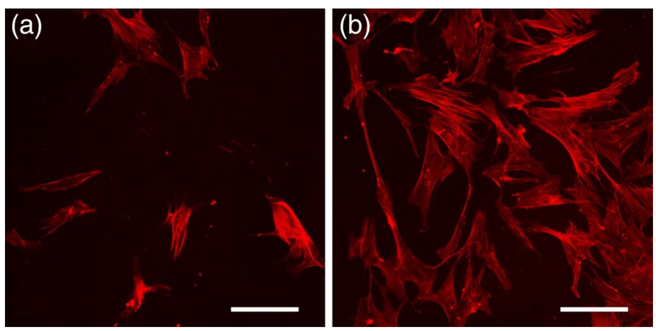

FIGURE 8 Fluorescence images of the (a) hMSCs and (b) hMSC incubated with the Janus base nanotube (JBNT)/fibronectin (FN) Nano-Matrix. Scale bar: 100 μm

Because cell morphology has been recognized as an indicator of cell functions and differentiation, we also quantified the cell morphological changes in this study. As shown in Figure 9, cell circularity showed a significant difference between the JBNT/FN Nano-Matrix group and the negative control group. Although cell roundness did not reach a specifically difference, it also shows a similar trend. The

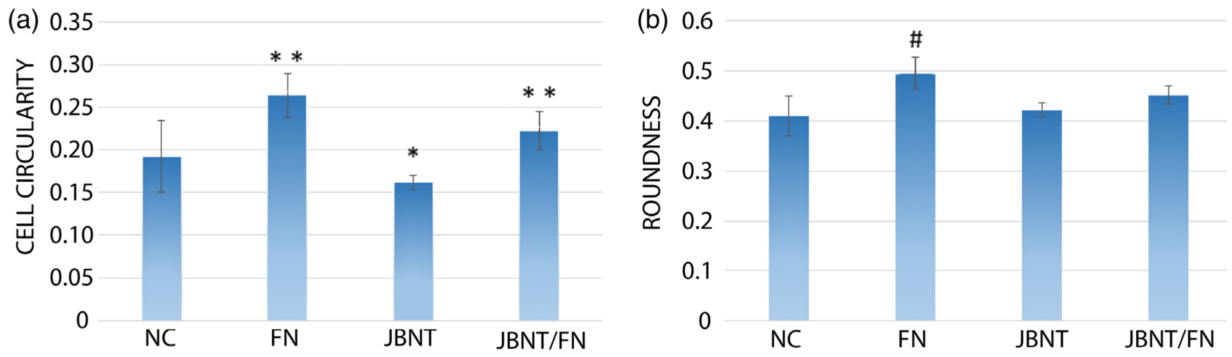

FIGURE 9 Statistical analysis of cell morphology. (a) Cell circularity. (b) Cell roundness. *$p < .05$ compared to negative controls (NCs). **$p < .05$ compared to Janus base nanotube (JBNT) alone. #$p < .05$ compared to JBNT alone. $N = 3$

significant difference of the circularity may reflect the differentiation of the cells (Rottmar, Lischer, Pleskova, Bruinink, & Maniura-Weber, 2009).

4 | DISCUSSION

In this article, we have developed a self-assembled Nano-Matrix, which may be served as a novel tissue engineering scaffold. Some bone or joint fractures happen in locations that are difficult to reach (Su et al., 2016; Sundararaj, Cieply, Gupta, Milbrandt, & Puleo, 2015). Although there are many established methods to fabricate tissue regenerative scaffolds, such as 3D print and electrostatic spinning technologies (Buttafoco et al., 2006; Do, Khorsand, Geary, & Salem, 2015; Shi et al., 2017; Yoshimoto, Shin, Terai, & Vacanti, 2003), a premade tissue scaffold with a specific shape is difficult to be implanted into these fracture sites that are deep in the joints. In contrast, our Nano-Matrix can be injected JBNT and FN solutions as liquid into the injured site and then self-assembled into a scaffold for cell anchorage and subsequent tissue regeneration. Important to note, although some hydrogels are injectable materials which can form a gel with a homogeneous surface and structure (Waghmare, Arora, Bhattacharjee, & Katti, 2018), they are different from the Nano-Matrix. The Nano-Matrix has a significant fibrous structure which more closely mimics the ECM.

The Nano-Matrix is biomimetic from two aspects: (a) JBNTs is formed from adenine–thymine Janus bases mimicking DNA bases. Moreover, JBNTs formed via hydrogen bonds instead of covalent bonds, so they present excellent biodegradability and biocompatibility (Chen et al., 2010). They have significant lower toxicity than covalent nanotubes such as carbon nanotubes (Journeay, Suri, Moralez, Fenniri, & Singh, 2008). (b) The assembly of Nano-Matrix is based on positive/negative charge interactions of JBNTs and FN. Moreover, because JBNTs mimic the morphology and the surface amine groups of collagen fibers. The self-assembly of JBNTs and FN is a biomimetic process mimicking FN and collagen assembly. Similar as JBNTs, the Nano-Matrix is also formed via no-covalent bound from JBNTs and FN, so it may also have superior biodegradability and biocompatibility compared with covalent scaffolds. Especially, unlike the crosslink of some polymers (Elbert & Hubbell, 2001; Mellott, Searcy, & Pishko, 2001; Trenor, Shultz, Love, & Long, 2004; Yeo et al., 2006), the assembly of JBNTs does not require any chemical additives or UV. Therefore, it does not have any toxic chemical residues.

Bone fractures can usually heal without difficulty in healthy young adults, but osteoporosis or older patients require a bioactive therapeutic to facilitate fracture healing. In our study, we used FN as important component to increase adhesion and migration of MSCs which can undergo osteogenic differentiation for improved bone fracture healing. FN is a ubiquitous multifunctional protein abundant in the ECM under dynamic remodeling conditions alongside with collagen and other glycoproteins. It has been proved to have an ability to accelerate the adhesion and migration of cells. During the bone healing process, FN presents a critical role in attracting MSCs to migrate to and adhere on the fracture location site is the first step in bone regeneration (Wang et al., 2019; Zhang, Hekmatfar, Ramanathan, & Karuri, 2013). Especially, FN can bind with cell surface integrin receptors. Previous studies have shown such bind may also positively influence stem cell differentiation and functions (Arnold et al., 2004; Keselowsky, Collard, & Garcia, 2003; Martino et al., 2009).

Our JBNT/FN Nano-Matrix is designed morphologically and functionally mimic the interaction of FN and collagen so that it not only can serve as structural support for tissues but also has the capability to support hMSC accumulation in a repair site by enhancing cell adhesion and migration after the cells have been signaled to home to the injury site, revealing its great potential as a novel scaffold for stem cell anchorage. Adhesion is the first step for cell growth and functions. Excellent adhesion and spread cell morphology indicate a successful anchorage which is important for subsequent cell growth and functions (Aplin, Howe, Alahari, & Juliano, 1998; Folkman & Moscona, 1978). In this study, our main purpose is to develop a novel self-assembled scaffold for stem cell anchorage. Although we got some indications from the cell morphology studies (Figures 8 and 9) that improved MCS adhesion may contribute to their osteogenic differentiation (as other studies also noticed (Rocca et al., 2015; Uynuk-Ool et al., 2017)), we have not confirmed these results. As a future study, we will test MSC differentiation on our Nano-Matrix.

5 | CONCLUSION

In conclusion, we fabricated a novel self-assembled biomimetic Nano-Matrix with DNA based nanotubes JBNTs and glycoprotein FN. In our experiment, we have shown that the Nano-Matrix has improved the migration and adhesion of the hMSCs. The Nano-Matrix has the capability to work in conjunction with chemical or molecular signals that trigger MSC anchorage by enhancing cell adhesion and migration once the cells are recruited. We envision the injectable Nano-Matrix will enhance targeted repair and serve as a scaffold for MSCs anchorage to a fracture site. Based on the hydrophobic core of the JBNTs, the Nano-Matrix also presents the potential to serve as hydrophobic drugs carrier within the core, which will be explored in subsequent experiments.

ACKNOWLEDGMENTS

This work is funded by National Institutes of Health (NIH) (grants 1R01AR072027-01 and 1R03AR069383-01), NSF Career Award (1653702), and University of Connecticut.

CONFLICT OF INTEREST

Y.C. is a cofounder of NanoDe Therapeutics, Inc.

ORCID

Yupeng Chen https://orcid.org/0000-0001-6940-6277

REFERENCES

Aplin, A. E., Howe, A., Alahari, S. K., & Juliano, R. L. (1998). Signal transduction and signal modulation by cell adhesion receptors: The role of integrins, cadherins, immunoglobulin-cell adhesion molecules, and selectins. *Pharmacological Reviews*, *50*(2), 197–263.

Arnold, M., Cavalcanti-Adam, E. A., Glass, R., Blummel, J., Eck, W., Kantlehner, M., … Spatz, J. P. (2004). Activation of integrin function by nanopatterned adhesive interfaces. *ChemPhysChem*, *5*(3), 383–388.

Buttafoco, L., Kolkman, N. G., Engbers-Buijtenhuijs, P., Poot, A. A., Dijkstra, P. J., Vermes, I., & Feijen, J. (2006). Electrospinning of collagen and elastin for tissue engineering applications. *Biomaterials*, *27*(5), 724–734.

Chen, Q.; Yu, H.C.; Chen, Y.P. (2017). *U.S. Patent No*. 20170362238A1, Rhode Island Hospital. https://patents.google.com/patent/US20170362238A1/en?inventor=yupeng+chen&oq=yupeng+chen.

Chen, Y., Bilgen, B., Pareta, R. A., Myles, A. J., Fenniri, H., Ciombor, D. M., … Webster, T. J. (2010). Self-assembled rosette nanotube/hydrogel composites for cartilage tissue engineering. *Tissue Engineering. Part C: Methods*, *16*(6), 1233–1243.

Chen, Y., Song, S., Yan, Z., Fenniri, H., & Webster, T. J. (2011). Self-assembled rosette nanotubes encapsulate and slowly release dexamethasone. *International Journal of Nanomedicine*, *6*, 1035–1044.

Danial, M., Tran, C. M., Young, P. G., Perrier, S., & Jolliffe, K. A. (2013). Janus cyclic peptide-polymer nanotubes. *Nature Communications*, *4*, 2780.

de Barros, A. P., Takiya, C. M., Garzoni, L. R., Leal-Ferreira, M. L., Dutra, H. S., Chiarini, L. B., … Rossi, M. I. (2010). Osteoblasts and bone marrow mesenchymal stromal cells control hematopoietic stem cell migration and proliferation in 3D in vitro model. *PLoS One*, *5*(2), e9093.

De Becker, A., & Riet, I. V. (2016). Homing and migration of mesenchymal stromal cells: How to improve the efficacy of cell therapy? *World Journal of Stem Cells*, *8*(3), 73–87.

Do, A. V., Khorsand, B., Geary, S. M., & Salem, A. K. (2015). 3D printing of scaffolds for tissue regeneration applications. *Advanced Healthcare Materials*, *4*(12), 1742–1762.

Elbert, D. L., & Hubbell, J. A. (2001). Conjugate addition reactions combined with free-radical cross-linking for the design of materials for tissue engineering. *Biomacromolecules*, *2*(2), 430–441.

Erickson, H. P., Carrell, N., & McDonagh, J. (1981). Fibronectin molecule visualized in electron microscopy: A long, thin, flexible strand. *Journal of Cell Biology*, *91*(3 Pt. 1), 673–678.

Fenniri, H., Mathivanan, P., Vidale, K. L., Sherman, D. M., Hallenga, K., Wood, K. V., & Stowell, J. G. (2001). Helical rosette nanotubes: Design, self-assembly, and characterization. *Journal of the American Chemical Society*, *123*(16), 3854–3855.

Folkman, J., & Moscona, A. (1978). Role of cell shape in growth control. *Nature*, *273*(5661), 345–349.

Gibon, E., Lu, L., & Goodman, S. B. (2016). Aging, inflammation, stem cells, and bone healing. *Stem Cell Research & Therapy*, *7*, 44.

Hadjiargyrou, M., & O'Keefe, R. J. (2014). The convergence of fracture repair and stem cells: Interplay of genes, aging, environmental factors and disease. *Journal of Bone and Mineral Research*, *29*(11), 2307–2322.

Johnell, O., & Kanis, J. A. (2006). An estimate of the worldwide prevalence and disability associated with osteoporotic fractures. *Osteoporosis International*, *17*(12), 1726–1733.

Jones, M., & Leroux, J. (1999). Polymeric micelles - a new generation of colloidal drug carriers. *European Journal of Pharmaceutics and Biopharmaceutics*, *48*(2), 101–111.

Journeay, W. S., Suri, S. S., Moralez, J. G., Fenniri, H., & Singh, B. (2008). Rosette nanotubes show low acute pulmonary toxicity in vivo. *International Journal of Nanomedicine*, *3*(3), 373–384.

Karp, J. M., & Leng Teo, G. S. (2009). Mesenchymal stem cell homing: The devil is in the details. *Cell Stem Cell*, *4*(3), 206–216.

Keselowsky, B. G., Collard, D. M., & Garcia, A. J. (2003). Surface chemistry modulates fibronectin conformation and directs integrin binding and specificity to control cell adhesion. *Journal of Biomedical Materials Research. Part A*, *66*(2), 247–259.

Manolagas, S. C., & Parfitt, A. M. (2010). What old means to bone. *Trends in Endocrinology and Metabolism*, *21*(6), 369–374.

Martino, M. M., Mochizuki, M., Rothenfluh, D. A., Rempel, S. A., Hubbell, J. A., & Barker, T. H. (2009). Controlling integrin specificity and stem cell differentiation in 2D and 3D environments through regulation of fibronectin domain stability. *Biomaterials*, *30*(6), 1089–1097.

Mellott, M. B., Searcy, K., & Pishko, M. V. (2001). Release of protein from highly cross-linked hydrogels of poly(ethylene glycol) diacrylate fabricated by UV polymerization. *Biomaterials*, *22*(9), 929–941.

Ogura, N., Kawada, M., Chang, W. J., Zhang, Q., Lee, S. Y., Kondoh, T., & Abiko, Y. (2004). Differentiation of the human mesenchymal stem cells derived from bone marrow and enhancement of cell attachment by fibronectin. *Journal of Oral Science*, *46*(4), 207–213.

Rocca, A., Marino, A., Rocca, V., Moscato, S., de Vito, G., Piazza, V., … Ciofani, G. (2015). Barium titanate nanoparticles and hypergravity stimulation improve differentiation of mesenchymal stem cells into osteoblasts. *International Journal of Nanomedicine*, *10*, 433–445.

Rottmar, M., Lischer, S., Pleskova, M., Bruinink, A., & Maniura-Weber, K. (2009). Correlating cell architecture with osteogenesis: First steps towards live single cell monitoring. *European Cells & Materials*, *18*, 59–62.

Shi, W., Sun, M., Hu, X., Ren, B., Cheng, J., Li, C., … Ao, Y. (2017). Structurally and functionally optimized silk-fibroin-gelatin scaffold using 3D printing to repair cartilage injury in vitro and in vivo. *Advanced Materials*, *29*(29), 1701089.

Singh, P., & Schwarzbauer, J. E. (2012). Fibronectin and stem cell differentiation—Lessons from chondrogenesis. *Journal of Cell Science*, *125*(Pt. 16), 3703–3712.

Somaiah, C., Kumar, A., Mawrie, D., Sharma, A., Patil, S. D., Bhattacharyya, J., … Jaganathan, B. G. (2015). Collagen promotes higher adhesion, survival and proliferation of mesenchymal stem cells. *PLoS One*, *10*(12), e0145068.

Song, S., Chen, Y., Yan, Z., Fenniri, H., & Webster, T. J. (2011). Self-assembled rosette nanotubes for incorporating hydrophobic drugs in physiological environments. *International Journal of Nanomedicine*, *6*, 101–107.

Su, Y. W., Chung, R., Ruan, C. S., Chim, S. M., Kuek, V., Dwivedi, P. P., … Xian, C. J. (2016). Neurotrophin-3 induces BMP-2 and VEGF activities and promotes the bony repair of injured growth plate cartilage and bone in rats. *Journal of Bone and Mineral Research*, *31*(6), 1258–1274.

Sui, B. D., Hu, C. H., Zheng, C. X., & Jin, Y. (2016). Microenvironmental views on mesenchymal stem cell differentiation in aging. *Journal of Dental Research*, *95*(12), 1333–1340.

Sundararaj, S. K., Cieply, R. D., Gupta, G., Milbrandt, T. A., & Puleo, D. A. (2015). Treatment of growth plate injury using IGF-I-loaded PLGA scaffolds. *Journal of Tissue Engineering and Regenerative Medicine*, *9*(12), E202–E209.

Trenor, S. R., Shultz, A. R., Love, B. J., & Long, T. E. (2004). Coumarins in polymers: From light harvesting to photo-cross-linkable tissue scaffolds. *Chemical Reviews*, *104*(6), 3059–3077.

Uynuk-Ool, T., Rothdiener, M., Walters, B., Hegemann, M., Palm, J., Nguyen, P., … Rolauffs, B. (2017). The geometrical shape of mesenchymal stromal cells measured by quantitative shape descriptors is determined by the stiffness of the biomaterial and by cyclic tensile forces. *Journal of Tissue Engineering and Regenerative Medicine*, *11*(12), 3508–3522.

van den Bogaerdt, A. J., van der Veen, V. C., van Zuijlen, P. P., Reijnen, L., Verkerk, M., Bank, R. A., … Ulrich, M. M. (2009). Collagen cross-linking by adipose-derived mesenchymal stromal cells and scar-derived mesenchymal cells: Are mesenchymal stromal cells involved in scar formation? *Wound Repair and Regeneration*, *17*(4), 548–558.

Veevers-Lowe, J., Ball, S. G., Shuttleworth, A., & Kielty, C. M. (2011). Mesenchymal stem cell migration is regulated by fibronectin through alpha5beta1-integrin-mediated activation of PDGFR-beta and potentiation of growth factor signals. *Journal of Cell Science*, *124*(Pt 8), 1288–1300.

Waghmare, N. A., Arora, A., Bhattacharjee, A., & Katti, D. S. (2018). Sulfated polysaccharide mediated TGF-beta1 presentation in pre-formed injectable scaffolds for cartilage tissue engineering. *Carbohydrate Polymers*, *193*, 62–72.

Wang, P., Hu, Z., Cao, X., Huang, S., Dong, Y., Cheng, P., … Zhu, J. (2019). Fibronectin precoating wound bed enhances the therapeutic effects of autologous epidermal basal cell suspension for full-thickness wounds by improving epidermal stem cells' utilization. *Stem Cell Research & Therapy*, *10*(1), 154.

Yao, W., Lay, Y. E., Kot, A., Liu, R., Zhang, H., Chen, H., … Lane, N. E. (2016). Improved mobilization of exogenous mesenchymal stem cells to bone for fracture healing and sex difference. *Stem Cells*, *34*(10), 2587–2600.

Yeo, Y., Burdick, J. A., Highley, C. B., Marini, R., Langer, R., & Kohane, D. S. (2006). Peritoneal application of chitosan and UV-cross-linkable chitosan. *Journal of Biomedical Materials Research. Part A*, *78*(4), 668–675.

Yoshimoto, H., Shin, Y. M., Terai, H., & Vacanti, J. P. (2003). A biodegradable nanofiber scaffold by electrospinning and its potential for bone tissue engineering. *Biomaterials*, *24*(12), 2077–2082.

Zhang, C., Hekmatfar, S., Ramanathan, A., & Karuri, N. W. (2013). PEGylated human plasma fibronectin is proteolytically stable, supports cell adhesion, cell migration, focal adhesion assembly, and fibronectin fibrillogenesis. *Biotechnology Progress*, *29*(2), 493–504.

SUPPORTING INFORMATION

Additional supporting information may be found online in the Supporting Information section at the end of this article.

How to cite this article: Zhou L, Yau A, Yu H, Kuhn L, Guo W, Chen Y. Self-assembled biomimetic Nano-Matrix for stem cell anchorage. *J Biomed Mater Res*. 2020;1–8. https://doi.org/10.1002/jbm.a.36875